JB Journals.ASM.org

PilMNOPQ from the *Pseudomonas aeruginosa* Type IV Pilus System Form a Transenvelope Protein Interaction Network That Interacts with PilA

Stephanie Tammam,[a,b] Liliana M. Sampaleanu,[a] Jason Koo,[a,b] Kumararaaj Manoharan,[a] Mark Daubaras,[a] Lori L. Burrows,[c] P. Lynne Howell[a,b]

Program in Molecular Structure and Function, Research Institute, The Hospital for Sick Children, Toronto, Ontario, Canada[a]; Department of Biochemistry, University of Toronto, Ontario, Canada[b]; Department of Biochemistry and Biomedical Sciences, McMaster University, Hamilton, Ontario, Canada[c]

***Pseudomonas aeruginosa* type IV pili (T4P) are virulence factors that promote infection of cystic fibrosis and immunosuppressed patients. As the absence of T4P impairs colonization, they are attractive targets for the development of novel therapeutics. Genes in the *pilMNOPQ* operon are important for both T4P assembly and a form of bacterial movement, called twitching motility, that is required for pathogenicity. The type II membrane proteins, PilN and PilO, dimerize via their periplasmic domains and anchor this complex in the inner membrane. Our earlier work showed that PilNO binds PilP, a periplasmic lipoprotein (S. Tammam, L. M. Sampaleanu, J. Koo, P. Sundaram, M. Ayers, P. A. Chong, J. D. Forman-Kay, L. L. Burrows, and P. L. Howell, Mol. Microbiol. 82:1496–1514, 2011). Here, we show that PilP interacts with the N0 segment of the outer membrane secretin PilQ via its C-terminal domain, and that the N-terminal cytoplasmic tail of PilN binds to the actin-like protein PilM, thereby connecting all cellular compartments via the PilMNOPQ protein interaction network. We show that PilA, the major pilin subunit, interacts with PilNOPQ. The results allow us to propose a model whereby PilA makes extensive contacts with the transenvelope complex, possibly to increase local concentrations of PilA monomers for polymerization. The PilNOP complex could provide a stable anchor in the inner membrane, while the PilMNOPQ transenvelope complex facilitates transit of the pilus through the periplasm and clamps the pilus in the cell envelope. The PilMN interaction is proposed to be responsible for communicating signals from the cytoplasmic to periplasmic components of this complex macromolecular machine.**

Type IV pili (T4P) are surface appendages involved in many processes, including adhesion to biotic and abiotic surfaces, aggregation, DNA uptake, and twitching motility (1–3). T4P are essential virulence factors that have been extensively studied in the model organism *P. aeruginosa* and other bacteria. Since adhesion and twitching motility play important roles in pathogenicity, understanding structure/function relationships involved in T4P assembly is vital for the development of novel therapeutic strategies to combat infection.

The intricacies of the T4P machinery are puzzling, and a comprehensive understanding of how these thin filaments are rapidly extended and retracted while resisting mechanical forces upwards of 100 pN (4) remains elusive. On a macromolecular scale, the machine has a modular organization with four subcomplexes: the cytoplasmic motor subcomplex (consisting of PilB, PilT, PilU, PilC, and, potentially, PilD), the inner membrane alignment subcomplex (PilM, PilN, PilO, and PilP), the outer membrane secretin pore subcomplex (PilQ and PilF), and the pilus itself (PilA and the minor pilins) (5). The dynamics of PilA (pilin) polymerization/depolymerization rely on the action of the motor ATPases PilB (pilus extension), PilT and PilU (pilus retraction), and the integral membrane protein PilC, the putative platform protein. T4P exit the cell through the secretin, which is comprised of multiple PilQ monomers (6). Assembly of the PilQ secretin requires its cognate pilotin (a protein essential for assembly of the secretin in the outer membrane), PilF (7). Bridging the cytoplasmic and outer membrane components is the alignment complex comprised of PilMNOP (8). PilM is a cytoplasmic actin-like protein that has been shown in *Thermus thermophilus* to bind the N terminus of PilN (9), while the cytoplasmic domain of the PilM homolog in the type 2 secretion system (T2SS) interacts with the single ATPase and the PilC homolog (10). PilN is a type II membrane protein that heterodimerizes with PilO, a protein with a similar domain organization (11). The periplasmic domains of PilNO interact with the inner membrane lipoprotein PilP, forming a 1:1:1 complex (12). The pilus is composed of hundreds of copies of PilA, as well as low-abundance pilin-like proteins, termed minor pilins (13).

While there are significant structural and functional similarities between components of T4P and T2SS assembly machineries (14–16), there are a few notable differences. For example, PilM and PilN appear to be the structural and functional equivalents of the cytoplasmic and periplasmic portions, respectively, of the T2SS protein EpsL (17). However, while PilM has been demonstrated to bind ATP, the cytoplasmic domain of EpsL does not (18). Also, EpsL interacts with the hexameric ATPase EpsE (19, 20), an interaction that has not yet been demonstrated for PilM and the equivalent ATPase PilB. There is further structural similarity between the T4P inner membrane lipoprotein PilP and the

Received 11 January 2013 Accepted 22 February 2013
Published ahead of print 1 March 2013
Address correspondence to P. Lynne Howell, howell@sickkids.ca, or Lori L. Burrows, burrowl@mcmaster.ca.
Supplemental material for this article may be found at http://dx.doi.org/10.1128/JB.00032-13.

doi:10.1128/JB.00032-13

HR region of the T2SS inner membrane protein, GspC (12, 21, 22). Here, we highlight a unique structural difference between PilP and GspC that may reflect a role of the transenvelope complex in retraction of long extracellular pili.

The current study expands our understanding of the role of PilMNOPQ in T4P assembly. We demonstrate that the cytoplasmic extension of *P. aeruginosa* PilN interacts directly with PilM, consistent with structural and bacterial two-hybrid data from *T. thermophilus* and *Neisseria meningitis*, respectively (9, 23). Further, we show that in *P. aeruginosa*, the N-terminal disordered domain of PilP interacts with the periplasmic regions of PilNO, while the C-terminal β-domain of PilP interacts with the N0 domain of PilQ, further refining the boundaries of the PilP-PilQ interaction identified in *N. meningitidis* (24). We show that PilNO have no affinity for PilQ under our experimental conditions, but that PilP interacts with both PilNO and PilQ, allowing all four proteins to be copurified using 6×His-tagged PilQ as bait. Together, these data suggest that PilP connects the inner and outer membrane subcomplexes. We also demonstrate that PilQ is able to pull down PilN, PilO, PilP, and PilA from PAO1 (a well-characterized *P. aeruginosa* strain) lysates, indicating that PilA (and possibly the pilus itself) forms multiple interactions with the transenvelope complex formed by PilMNOPQ.

MATERIALS AND METHODS

Bacterial strains. Table S1 in the supplemental material summarizes the bacterial strains and vectors used in this study. The pET-Duet and pET vectors were transformed by heat shock into chemically competent *Escherichia coli*.

Western blot analysis. All protein samples analyzed by Western blotting were mixed with 2× SDS-PAGE sample buffer at a 1:1 ratio, boiled for 10 min, separated on 16% SDS-PAGE minigels, and transferred to polyvinylidene difluoride (PVDF) membranes. Proteins of interest were detected using the purified rabbit polyclonal antibodies to PilMNOPQA (8). The primary antibodies were diluted in TBST (25 mM Tris-HCl, pH 7.5, 150 mM NaCl, and 0.1% [vol/vol] Tween 20). The secondary anti-rabbit or anti-mouse antibodies conjugated to alkaline phosphatase were used per the manufacturer's instructions (Bio-Rad), and the blots were developed with nitroblue tetrazolium/5-bromo-4-chloro-3-indoyl-phosphate (NBT/BCIP) from BioShop Canada Inc. Detection of the biotinylated PilN_N20 peptide was performed using the streptavidin-horseradish peroxidase-conjugated reagent (Strep-HRP) from GenScript in TBST, followed by detection of HRP using the Super Signal West Pico chemiluminescent substrate from Pierce (Thermo Scientific).

Construct generation and peptide synthesis. (i) PilN N-terminal peptides. The peptides encompassing the N-terminal 20 amino acids of PilN, MARINLLPWREELREQRKQQ (PilN_N20; 95% pure and reconstituted in water at 1 mg/ml) and the Asp5-to-Ala variant (PilN_N20_N5A; 86% purity) were synthesized by GenScript. For both wild-type and mutant PilN_N20 peptides, a lysine residue and a mini-PEG linker were added at the C terminus to facilitate the addition of a biotin molecule.

(ii) Generation of heterologous protein expression vectors. The generation of the coexpression vector that produces N-terminally 6×His-tagged $PilN_{\Delta 44}$ and untagged $PilO_{\Delta 51}$ ($PilN_{\Delta 44}/PilO_{\Delta 51}$), as well as the expression vectors for the 6×His-tagged proteins $PilO_{\Delta 43}$ and PilM or the untagged $PilP_{\Delta 18}$ ($PilP_{\Delta 18T7}$), were reported previously (8, 11, 12). Details about these vectors are shown in Table S1 in the supplemental material. The untagged versions N- and C-terminal constructs of PilP ($PilP_{18\text{-}84T7}$ and $PilP_{\Delta 71\_TAAT}$, respectively) were generated using $PilP_{\Delta 18T7}$ as a template to amplify the appropriate regions and subsequently ligated into the BamI and XhoI sites of pET24a. The PilQ expression constructs were amplified with specific primers containing a 5′ NcoI site and a 3′ XhoI site. Purified PCR fragments were digested and ligated into an appropriately digested pET28a vector. Clones were verified by sequencing (The Centre for Applied Genomics [TCAG] or the Analytical Genetics Technology Centre [AGTC], Toronto, Ontario, Canada).

Protein expression. PilM, $PilN_{\Delta 44}/PilO_{\Delta 51}$, $PilP_{\Delta 18}$, $PilP_{\Delta 71}$, and the PilQ constructs used in pulldown studies were expressed in *E. coli*. The pET vectors containing the genes of interest were transformed into BL21 Codon Plus cells (Stratagene) and plated on LB plates supplemented with 50 mg/ml kanamycin. One colony was then used to inoculate 5 ml LB containing the appropriate antibiotic (termed LB-antibiotic). Each overnight culture was used to inoculate 500 ml of LB-antibiotic, and the cells were grown at 37°C until an optical density at 600 nm (OD_{600}) of 0.6 to 0.7, when protein expression was induced by adding isopropyl-β-D-thiogalactopyranoside (IPTG) to a final concentration of 1.0 mM. The cells were allowed to grow either overnight at 18°C or for 4 h at 37°C prior to being harvested by centrifugation (7,700 × *g*, 30 min, 4°C). Cell pellets were stored at −20°C until required.

Bioinformatics analyses. (i) PilQ domain identification. Sequence alignments were performed by T-Coffee (25). Initially the sequences for the T2SS and T4P secretins were aligned separately. These individual alignments were subsequently combined using the COMBINE algorithm in the T-Coffee suite and then manipulated manually to refine the alignment in JalView (26). Secondary structure predictions were performed by JnetPRED (27) in the JalView alignment editor program (26). Figures for sequence alignments were produced in JalView. Structural analysis and alignments were performed using PyMOL (28).

(ii) PilP and GspC structural comparison. Sequence alignments were performed as described in reference 12, and structural superpositions were performed and displayed using PyMOL (28).

PilM copurification with PilN_N20 and PilN_N20_N5A peptides. N-terminally 6×His-tagged PilM ($PilM_{Nt6\times His}$) was copurified with PilN_N20 peptides using Ni MagBeads (GenScipt). Initially, 0.2 g of dry $PilM_{Nt6\times His}$ pellet was solubilized in 4 ml Easy BacLysis buffer (GenScript) and 2 ml buffer A (20 mM Tris-HCl, pH 7.5, 150 mM NaCl) with 100 mg/ml lysozyme, 10 mg/ml DNase, and 10 mg/ml RNase. Cells were lysed by incubation for 1 h at 4°C on a rotator. Subsequently, 2 ml of cell lysate solution was added to each of the three falcon tubes containing 100 μl of Ni MagBeads preequilibrated in lysis buffer. After mixing for 1.5 h at room temperature on a rotator, the falcon tubes were inserted in the magnetic base and the supernatant was discarded. The MagBeads with bound $PilM_{Nt6\times His}$ were then incubated with either 1 ml of buffer A alone (control) or 1 ml buffer A and 100 μl of 1 mg/ml wild-type PilN_N20 or mutant PilN_N20_N5A peptide (freshly made solutions of lyophilized synthetic peptides in water). The control experiments of both PilN peptides in the absence of PilM were set up in a similar manner. After an overnight incubation at 4°C on a rotator, the Ni-NTA beads were washed in a batch-wise manner using the magnetic base, and the 1.1-ml flow-through, together with 3-, 3-, 0.5-, 0.5-, and 0.5-ml elute fractions, containing 10, 30, 75, 150, or 400 mM imidazole, respectively, were collected and analyzed by SDS-PAGE and Western blotting using both anti-PilM antibody and a Strep-HRP reagent.

PilN/O and PilP N-terminal pulldowns. The expression, lysis, copurification, and analysis of pulldowns were performed as described in Tammam et al. (12) for the $PilN_{\Delta 44}/PilO_{\Delta 51}/PilP_{\Delta 18\_6\times His}$ cofractionation. In brief, the pET28a-*pilP*$_{\Delta 18\text{-}6His}$ and pET-Duet-*pilN*$_{\Delta 44}$-*pilO*$_{\Delta 51}$ expression vectors were transformed separately into *E. coli* BL21(DE3) cells (Novagen). Overnight cultures were used to inoculate 1 liter of LB-kanamycin, and cells were grown at 37°C until an OD_{600} of 0.6 to 0.7, when protein expression was induced by adding IPTG to a final concentration of 1 mM. The cells were grown for 4 h after induction at 37°C, harvested by centrifugation, and stored at −20°C until required. The frozen cells were thawed, resuspended, and then mixed together. The cells were lysed by homogenization, and the cellular debris was removed by centrifugation. The cell lysate was mixed with 2 ml of Ni-agarose (Qiagen) at 4°C for 2 h and then packed into a column and washed twice with 20 ml of Tris buffer contain-

ing, successively, 10 and 30 mM imidazole. Bound protein was eluted from the column in three 10-ml batches with Tris buffer and 75, 150, and 300 mM imidazole, respectively. The 75 mM imidazole fraction was subsequently concentrated to 2 ml (Amicon unit with 10-kDa cutoff; Millipore), to a final protein concentration of 10 to 15 mg/ml. The concentrated protein sample was applied to a Superdex S-200 column (GE Health) and eluted using 20 mM Tris-HCl, pH 7.5, and 150 mM NaCl.

PilQ pulldown experiments. All proteins were overexpressed as described above. Each protein construct was expressed individually, and appropriate cell pellets were then mixed prior to lysis. $PilP_{\Delta 18}$, $PilP_{\Delta 71}$, $PilN_{\Delta 44}/PilO_{\Delta 51}$, $PilQ_{24\text{-}445}$, $PilQ_{24\text{-}280}$, $PilQ_{281\text{-}445}$, $PilQ_{281\text{-}410}$, and $PilQ_{281\text{-}376}$ were used in 0.5-liter aliquots, while 1-liter aliquots of $PilQ_{377\text{-}445}$ were used.

Individual cell pellets were initially resuspended in 10 ml of lysis buffer (50 mM Tris, pH 7.5, 150 mM NaCl, 5 mM imidazole, 1 mM phenylmethylsulfonyl fluoride [PMSF], 0.1 mg/ml DNase, RNase, lysozyme, and protease inhibitor cocktail [Sigma]). After mixing the appropriate resuspended pellets, cells were lysed by homogenization using an Avestin EmulsiFlex-C3 by passing the lysate three times through the machine at 15 to 20 kpsi. The insoluble debris was removed by centrifugation (39,000 × *g*, 30 min, 4°C). The cell lysate was then loaded on a preequilibrated Ni-NTA column, and the flowthrough was collected and loaded a second time on the column. The column was washed with 30 ml of buffer A containing 5 mM imidazole and a second wash of 10 ml buffer A with 30 mM imidazole. Bound protein was eluted from the column in three 10-ml batches with buffer A with 75, 150, and 300 mM imidazole, respectively. Fractions were analyzed by SDS-PAGE and Western blot analysis with PilN, PilO, PilP, and 6×His specific antibodies as appropriate.

Negative controls for $PilP_{\Delta 18\_TAAT}$, $PilP_{\Delta 71\_TAAT}$, and $PilN_{\Delta 44}/PilO_{\Delta 51}$ were run, where soluble lysate of cells overexpressing these constructs was loaded onto a Ni-NTA column in the absence of PilQ. Purification was carried out as described above, and the eluted fractions were analyzed by SDS-PAGE.

PilA pulldown assays. Cell pellets containing expressed $PilQ_{24\text{-}445}$, $PilQ_{24\text{-}280}$, and $PilQ_{281\text{-}445}$ were resuspended in 10 ml lysis buffer (as described above). Cells were lysed using an Avestin EmulsiFlex-C3 (as described above), and cellular debris was then removed by centrifugation (39,000 × *g*, 30 min, 4°C). The soluble supernatant was mixed with 1 ml Ni-NTA agarose (Qiagen), preequilibrated in buffer A, for 2 h at 4°C. The beads were collected by centrifugation, with the supernatant fraction being the flowthrough. The beads were washed once with 10 ml buffer A for 1 h at 4°C. The beads were again collected by centrifugation, resulting in Ni-NTA beads with prebound proteins that were subsequently used to pull down PilA from PAO1 lysates prepared as described below.

PAO1 cell lysates were prepared by growing cells streaked in a grid pattern on LB agar plates overnight at 37°C. Cells were collected by scraping them off the surface, and cell pellets were lysed in 6 ml Easy BacLysis and 14 ml buffer A with 100 mg/ml lysozyme, 10 mg/ml DNase, and 10 mg/ml RNase. Cell pellets were homogenized by brief vortexing and incubation at room temperature for 30 min on a rotator. Cellular debris was then removed by centrifugation (39,000 × *g*, 30 min, 4°C), and 4 ml of the cell lysate supernatant was applied to the Ni-NTA beads charged with specific His-tagged protein as described above.

The PAO1 cell lysates and Ni-NTA beads prebound with $PilQ_{24\text{-}445}$, $PilQ_{24\text{-}280}$, and $PilQ_{281\text{-}445}$ were incubated at 4°C overnight. The beads were collected by centrifugation, while the supernatant contained the flowthrough fraction. The resin was washed twice using a batch method (mixed for 1 h on a rotator at 4°C and centrifuged to pellet the beads and then remove the supernatants) with 10 ml buffer A containing, successively, 10 and 30 mM imidazole, and the bound proteins were eluted from the column in three 2-ml batches, containing buffer A and 75, 150, or 400 mM imidazole, respectively. The identity of each protein was confirmed by Western blotting of the flowthrough and 400 mM fractions using PilN-, PilO-, PilP-, and PilA-specific antibodies.

RESULTS

The conserved N terminus of PilN is important for T4P function and interacts with PilM *in vitro*. We previously identified the PilN N-terminal sequence $I_4N_5L_6L_7P_8$ as a signature sequence for PilN family members and predicted that this motif would be involved in interactions with PilM (11). To test this hypothesis, we examined the interaction of *P. aeruginosa* PilM and PilN using N-terminally tagged PilM ($PilM_{Nt6\times His}$) and a biotinylated peptide of PilN that contains the first 20 N-terminal residues of the protein conjugated via a C-terminal lysine and a mini-PEG linker to biotin (PilN_N20). This 2.5-kDa peptide copurified with $PilM_{Nt6\times His}$ using either nickel (Fig. 1) or streptavidin affinity chromatography (see Fig. S1 in the supplemental material). When HRP-conjugated streptavidin was used to probe the fractions from the nickel affinity purification, the biotinylated PilN_N20 peptide was recovered in the 10, 30, and 75 mM imidazole washes at ~40 kDa. Western blot analysis with an anti-6×His antibody confirmed that these bands correspond to PilM (Fig. 1A). In the presence of PilM, the PilN_N20 peptide appeared at the approximate molecular mass of PilM, indicating that this peptide forms a high-affinity interaction with $PilM_{Nt6\times His}$ that is not disrupted by SDS. In the absence of PilM, some peptide bound nonspecifically to the column (Fig. 1A), and under these conditions, the peptide eluted at ~2.5 kDa. However, when PilM was present, the levels of PilN_N20 in the high imidazole fractions were greatly diminished, presumably because most of the peptide is bound to PilM. Compared to the purification profile of PilM in the absence of the PilN peptide (Fig. 1C), it is clear that the addition of the peptide does not affect binding of PilM to the column. Together, these data suggest that PilN_N20 binds to PilM in the presence of SDS.

The effects of point mutations at the highly conserved Asn5 (N5A/Q/D) of PilN and a series of N-terminal deletions (Δ2-9, Δ10-18, and Δ4-17) were tested *in vivo* by complementation of a *P. aeruginosa pilN* mutant (*pilN*::FRT). Constructs expressing the PilN_N5A variant or deletion constructs lacking residues 2 to 9 or 4 to 18 did not restore twitching motility, phage sensitivity, or surface PilA in a *pilN* mutant (see Fig. S2 in the supplemental material). Other deletions and site-specific mutations decreased T4P biogenesis and function to various degrees (see Fig. S2). Mutations that prevent association of PilM and PilN *in vivo* were previously shown to lead to degradation of PilNO (8), consistent with the phenotypes seen here. When the pulldown experiments were repeated with a peptide containing the N5A mutation (PilN_N20_N5A), PilM was still pulled down (Fig. 1B), despite the *in vivo* data suggesting that this variant was nonfunctional (see Fig. S2) (23). Together, these data suggest that Asn5 in PilN plays an additional role in communicating a signal from the cytoplasm through PilN to the periplasmic components, or that the binding of PilM to the PilN peptide *in vivo* is influenced by other proteins or protein interactions that may be present.

The N terminus of PilP is sufficient for the interaction with PilNO. Previously, we showed that full-length PilP (minus its signal sequence) interacted with a stable complex of PilNO, and that the C-terminal β-sandwich domain of PilP alone could not bind PilNO (12). To directly probe the potential interaction of the N terminus of PilP with PilNO, a construct corresponding to the unstructured domain of PilP ($PilP_{19\text{-}84T7}$; 8.9 kDa) was used. Under the conditions used previously to characterize the interaction of mature PilP ($PilP_{\Delta 18\_6\times His}$) with the periplasmic PilNO

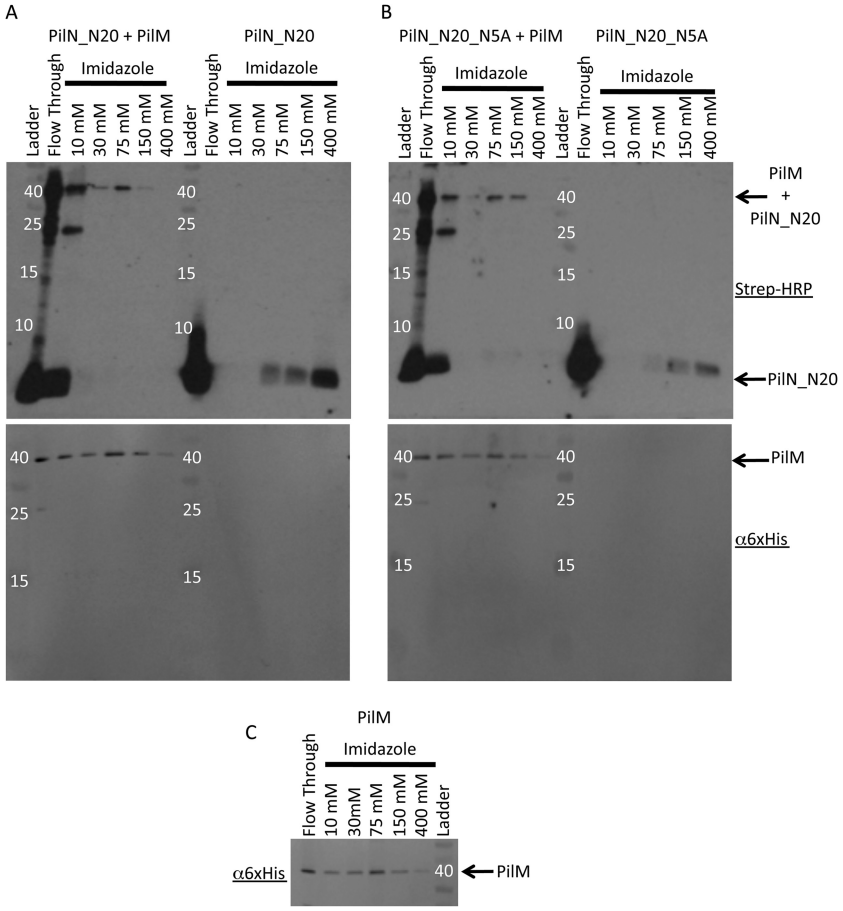

FIG 1 $PilM_{Nt6\times His}$ pulls down PilN_N20. (A) The wild-type PilN_N20 peptide binds to PilM in an SDS-resistant manner. Western blots were developed by enhanced chemiluminescence (ECL) with Strep-HRP, detecting biotinylated PilN_N20 peptide (top), and a blot was probed with a monoclonal 6×His antibody conjugated to alkaline phosphatase, probing for PilM, and detected by NBT-BCIP (bottom). (B) PilN_N20_N5A peptide binds to PilM in an SDS-resistant manner. The top and bottom panels are the same as those described for panel A. (C) Western blot probed with monoclonal 6×His antibody conjugated to alkaline phosphatase showing that PilM binds to the column in the absence of either PilN peptide, indicating that the binding of PilM to the Ni beads is not altered by the presence of the peptide. Ladder markers are labeled in kDa.

($PilN_{\Delta 44}/PilO_{\Delta 51}$) heterodimer (12), the PilP N-terminal construct cofractionated with PilNO, and this interaction was stable during size-exclusion chromatography (Fig. 2). Although the N-terminal PilP fragment was unstable when expressed in the absence of PilNO (see Fig. S3 in the supplemental material), it was protected from proteolytic degradation when in complex with PilNO. Examination of the $PilNOP_{19\text{-}84T7}$ complex by limited proteolysis suggested that the protected region of PilP spans residues

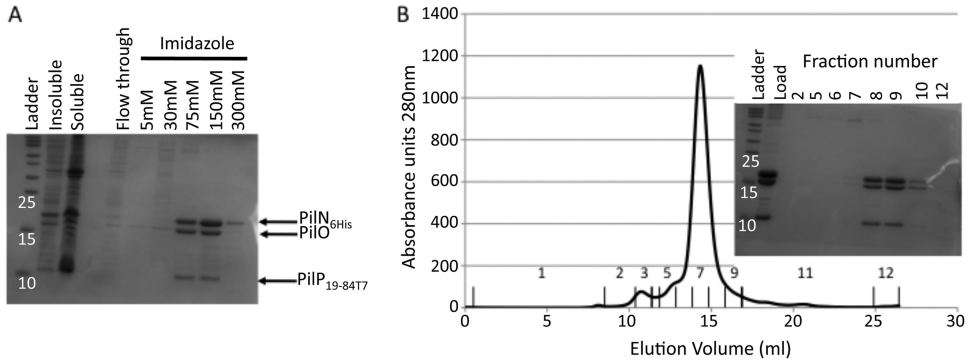

FIG 2 Copurification of PilNOP. (A) Coomassie-stained SDS-PAGE analysis of the $PilN_{\Delta 44\_6\times His}/PilO_{\Delta 51}/PilP_{19\text{-}84T7}$ fractions eluted from a Ni-NTA column in the presence of increasing imidazole concentrations. (B) Elution of the 75 mM imidazole Ni-NTA fraction shown in panel A from a Superdex 200 gel filtration column. The inset is the Coomassie-stained SDS-PAGE gel of the fractions from the gel filtration column.

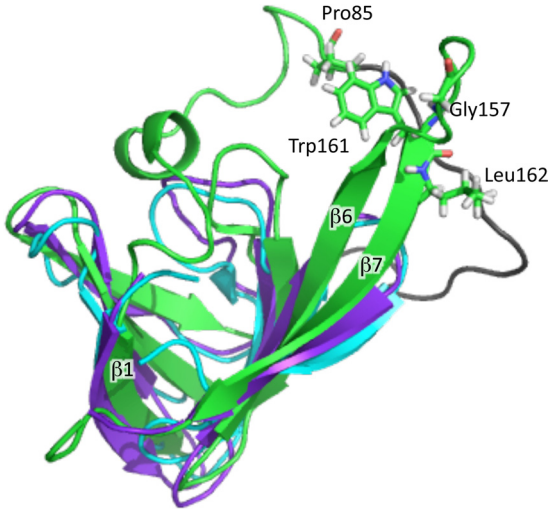

FIG 3 Structural comparison of PilP and GspC proteins. Cartoon representations of PilP (PDB code 2LC4; green), $GspC_{Dd}$ (PDB code 2LNV; cyan), and $GspC_{Ec}$ (PDB code 3OOS chain C; purple). For clarity, the following residues have been removed from the cartoon representations: $PilP_{\Delta 71}$, the C-terminal 6×His tag; $GspC_{Dd}$, the N-terminal residues 70 to 94 and the C-terminal residues 158 to 173; and $GspC_{Ec}$, the N-terminal residues 122 to 127. The location of the highly conserved Trp161 and residues selected for mutagenesis (Pro85, Gly157, and Leu162) in PilP are shown as sticks. The N-terminal β-strand, strand β1, and the two C-terminal strands, strands β6 and β7, have been labeled. The disordered N-terminal region of PilP is colored black.

19 to 76, a region that our bioinformatics analysis predicted to be entirely disordered (12). These data support our hypothesis that the N terminus of PilP mediates the interaction with PilNO (12).

An important structural difference between PilP and T2SS GspC HR region. Our earlier work highlighted a pair of highly conserved residues in PilP, Pro85 (found in the N-terminal disordered region) and Trp161 (found on β7), which interact and tether the N-terminal disordered region to the β-sandwich domain in solution (12). The recent release of two structures of the HR domain of the T2SS protein GspC from *E. coli* ($GspC_{Ec}$; Protein Data Bank [PDB] code 3OSS) and *Dickeya dadantii* 3937 ($GspC_{Dd}$; PDB code 2LNV) allowed us to extend our analysis of the PilP structure. The structures of $PilP_{\Delta 71}$ and $GspC_{Ec}$ or $GspC_{Dd}$ can be superimposed with root-mean-squared deviations of 0.92 and 1.5 Å over 51 and 43 C^{α} atoms, respectively (Fig. 3). The β-sandwich domains are very similar, but β-strands 6 and 7 in the GspC proteins are each two residues shorter than those in PilP (Fig. 3). Notably, this β6-β7 extension is the site of the highly conserved Trp residue (Trp161 in PilP) found in all PilP proteins. There is no equivalent conserved aromatic residue in the GspC family (data not shown). Mutation of Pro85 to either Ala or Glu, or the mutation of residues in the β6-β7 extension (Gly157 and Leu162), impaired *P. aeruginosa* twitching motility (see Fig. S4 in the supplemental material), indicating that this region of the protein is important for T4P biogenesis. However, in the case of the Pro85Val mutation, twitching was not diminished, reinforcing the notion that a hydrophobic interaction between the residue at this position and Trp161 is important for function. We propose that the interaction formed between Pro85 and Trp161 is important for stabilizing the relative orientations of the disordered N terminus and the β-sandwich domain, and that the β6-β7 extension and the Pro85-Trp161 interaction are T4P-specific adaptations for function.

The C terminus of PilP interacts with the periplasmic domain of PilQ. Genin and Boucher (29) analyzed a number of secretin sequences from the T2SS and T3SS and identified four highly conserved regions toward the C termini of the proteins that they termed secretin consensus regions. Alignments of PilQ protein sequences from various T4P-producing bacteria show the same conserved regions (see Fig. S5 in the supplemental material). Using these sequence alignments, we identified four discrete periplasmic domains in T4P secretins. The two N-terminal β-strand-rich domains share the lowest percent identity across PilQ homologues (Table 1; also see Fig. S5); thus, we termed these regions of PilQ the species-specific (SS) domains (SS1 and SS2). C terminal to the SS domains, we predicted that there are two additional domains that were recently confirmed to be structurally homologous to N0 and N1 from T2SS secretins (6), and we use that terminology here. From this analysis, we designed and expressed six soluble constructs spanning the periplasmic region of PilQ to examine the roles of these individual domains in more detail (Fig. 4). Briefly, these soluble constructs are $PilQ_{24\text{-}445}$ (containing the entire periplasmic domain), $PilQ_{24\text{-}280}$ (SS domains), $PilQ_{281\text{-}445}$ (N0 and N1), $PilQ_{281\text{-}410}$ (N0 and approximately one-third of N1), $PilQ_{281\text{-}376}$ (N0), and $PilQ_{377\text{-}445}$ (N1).

Each of the six 6×His-tagged constructs was tested for its ability to pull down untagged PilP from *E. coli* lysates. Three constructs of PilP were used: mature PilP ($PilP_{\Delta 18}$), the N-terminal region ($PilP_{19\text{-}84T7}$), and the C-terminal region ($PilP_{\Delta 71}$). $PilP_{19\text{-}84T7}$ was rapidly degraded after lysis, suggesting that no PilQ fragment could stabilize this region of PilP (see Fig. S3 in the supplemental material). In contrast, $PilP_{\Delta 18}$ and $PilP_{\Delta 71}$ were pulled down by three of the six soluble PilQ constructs (Fig. 5 and Table 2), while the negative control showed that the PilP fragments did not bind to the Ni-NTA column in the absence of PilQ (data not shown). $PilP_{\Delta 18}$ and $PilP_{\Delta 71}$ interacted with $PilQ_{281\text{-}445}$, $PilQ_{281\text{-}410}$, and $PilQ_{281\text{-}376}$, the three constructs containing the N0 domain at their N termini (Table 2). Together, these data suggest that the C-terminal β-domain region of PilP is sufficient for the interaction with PilQ, and that the site of PilP interaction with PilQ is the N0 domain.

TABLE 1 Summary of sequence identity and length of SS domains between *P. aeruginosa* PilQ and orthologues in other T4P systems[a]

PilQ ortholog	% Identity			Length of SS domain (no. of amino acids)
	Full length	SS domain only[b]	N0, N1, and secretin domains[c]	
NmPilQ	31	25	36	336
NgPilQ	32	28	35	298
FtPilQ	31	17	37	177
MxPilQ	31	21	39	478
RsPilQ	39	32	43	290

[a] The reference sequence is *P. aeruginosa* PilQ. NmPilQ, *N. meningitidis* PilQ; NgPilQ, *Neisseria gonorrhoeae* PilQ; FtPilQ, *Francisella tularensis* PilQ; MxPilQ, *Myxococcus xanthus* PilQ; RsPilQ, *Ralstonia solanacearum* PilQ.
[b] N-terminal boundaries used when calculating the percent identity: PaPilQ, residues 1 to 280; NmPilQ, residues 1 to 336; NgPilQ, residues 1 to 298; FtPilQ, residues 1 to 177; MxPilQ, residues 1 to 478; RsPilQ, residues 1 to 290.
[c] C-terminal boundaries used when calculating the percent identity: PaPilQ, residues 281 to 714; NmPilQ, residues 337 to 761; NgPilQ, residues 299 to 723; FtPilQ, residues 178 to 594; MxPilQ, residues 479 to 901; RsPilQ, residues 291 to 713.

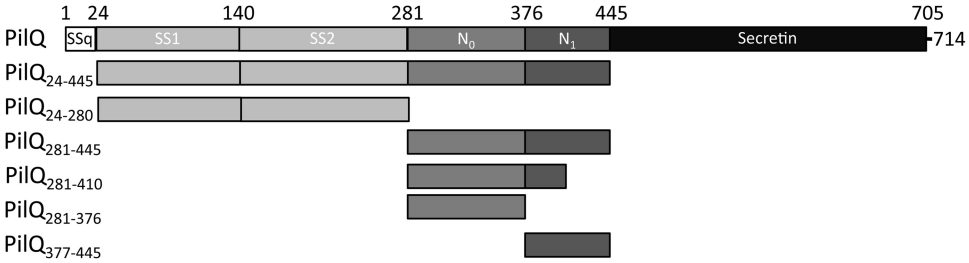

FIG 4 Schematic of soluble PilQ constructs. All constructs were cloned into pET28a with a C-terminal 6×His tag. Amino acid numbers are located above the schematic of the full-length protein. The first 24 residues are the signal peptidase signal sequence (SSq), residues 24 to 445 constitute the full periplasmic domain, and 445 to 714 the putative membrane-embedded secretin domain (Secretin). In the periplasm there are two distinct regions: residues 24 to 280 are the species-specific domain (SS), which can be divided into two subdomains (SS1, spanning residues 24 to 139, and SS2, spanning residues 140 to 280), while residues 281 to 445 share sequence and secondary structural homology with other secretins and have been found to play a role in multimerization. This multimerization domain can be divided into two subdomains, residues 281 to 376 and 377 to 445, corresponding to the highly conserved N0 and N1 domains, respectively.

Notably, the full-length periplasmic domain of PilQ ($PilQ_{24-445}$) did not pull down either $PilP_{\Delta 18}$ or $PilP_{\Delta 71}$ from cell lysates, even though this construct contains the N0 domain (Fig. 5B). It is possible that in this context *in vitro*, the binding site for PilP on the N0 domain is occluded. This PilQ periplasmic fragment may be conformationally flexible when expressed as a monomer *in vitro* but not as an oligomer *in vivo*, where its orientation would be constrained.

The PilNOP heterotrimer interacts with PilQ. Previously, we showed that PilP forms a stable heterotrimer with PilNO *in vitro* (12), and in this study we have shown that the extended N terminus of PilP interacts with PilNO, while its C-terminal β-domain interacts with PilQ. To test whether PilP could interact simultaneously with PilNO and PilQ, the pulldown experiments were repeated with all four proteins. PilNOP were pulled down by the same PilQ constructs that pulled down $PilP_{\Delta 18}$ and $PilP_{\Delta 71}$ (Table 2). Negative controls consisting of PilNO alone or PilNO with tagged PilQ constructs showed that PilNO was not retained on the column unless both PilP and tagged PilQ were present (Table 2). Therefore, PilP is sufficient to coordinate a stable interaction network between the inner membrane components PilNO and the outer membrane component PilQ.

PilA interacts with a PilNOPQ complex *in vivo*. Bacterial two-hybrid experiments using *N. meningitidis* T4P components expressed in *E. coli* indicated potential interactions of the major pilin subunit PilE (equivalent to PilA in *P. aeruginosa*) with spe-

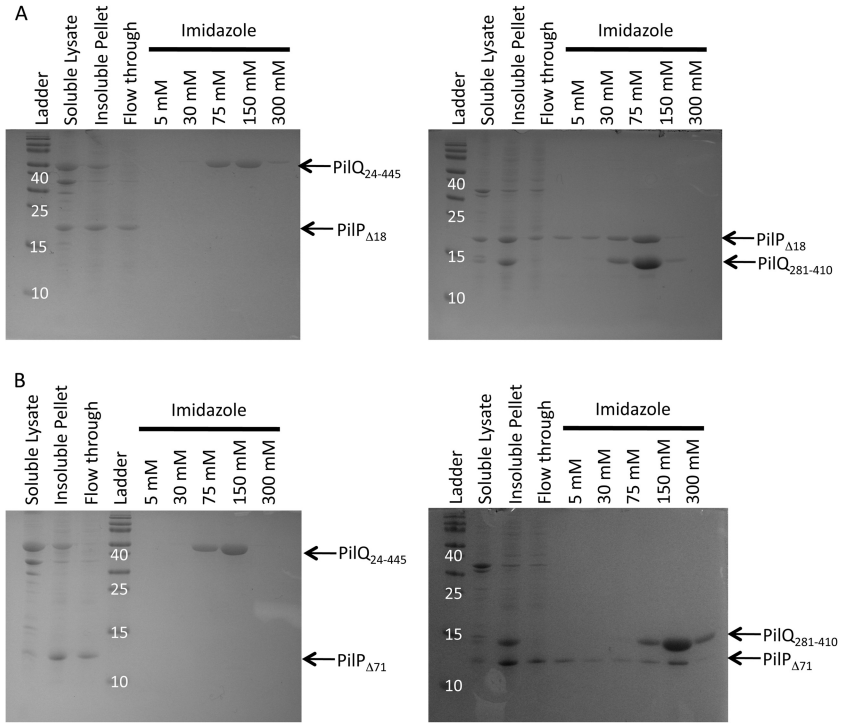

FIG 5 Cofractionation of PilP and PilQ from a Ni-NTA affinity column. (A) The Ni-NTA results of $PilP_{\Delta 18}$ and PilQ. The absence of any PilP in the high imidazole fractions when $PilQ_{24-445}$ is used as bait indicates that PilP is unable to interact with this construct, but when $PilQ_{281-445}$ is used as the bait protein, $PilP_{\Delta 18}$ is found in the high imidazole fractions. (B) The Ni-NTA results of $PilP_{\Delta 71}$ and PilQ. An interaction pattern similar to that observed for panel A is observed for $PilP_{\Delta 71}$. Ladder markers are labeled in kDa.

TABLE 2 Summary of protein-protein interactions with 6×His-tagged PilQ bait fragments

Fragment	$PilP_{\Delta 18}$	$PilP_{\Delta 71}$	PilN/O	$PilN/O/P_{\Delta 18}$
No bait	–[a]	–	–	–
$PilQ_{24-445}$	–	–	–	–
$PilQ_{24-280}$	–	–	–	–
$PilQ_{281-445}$	+	+	–	+
$PilQ_{281-410}$	+	+	–	+
$PilQ_{281-376}$	+	+	–	+
$PilQ_{377-445}$	–	–	–	–

[a] A minus sign indicates no interaction. A plus sign indicates an interaction in the pulldown assay.

cific inner membrane proteins (23). To test for potential interactions in *P. aeruginosa* and to include the periplasmic domains of PilQ, we performed a series of pulldown experiments using 6×His-tagged PilQ bait to capture prey proteins from detergent-solubilized *P. aeruginosa* lysates. Negative controls showed no interaction of proteins from detergent-solubilized PAO1 lysates with the Ni-NTA column (Fig. 6). In contrast, after extensive washing of the column, the bound $PilQ_{24-445}$, $PilQ_{24-280}$, or $PilQ_{281-445}$ fragments captured PilA from the lysates (Fig. 6). Western blots of imidazole eluates with antibodies specific to PilN, PilO, and PilP showed that PilQ captured all three proteins. Together, these data support formation of a stable PilNOPQ complex and suggest that PilA interacts with this complex. These data support the idea that PilA and/or the pilus make extensive contacts with the PilMNOPQ transenvelope complex.

DISCUSSION

This is the first report to provide evidence for a complete T4P transenvelope protein interaction network formed by the products of the *pilMNOPQ* operon. This complex has components in the cytoplasm (PilM), inner membrane (PilN, PilO, and PilP), and outer membrane (PilQ). This arrangement of the inner and outer membrane components of the pilus assembly complex may provide an unobstructed path through the periplasm, including the peptidoglycan, for the assembled pilus. Also, hypothesized interactions of PilM with the platform protein PilC, as demonstrated for orthologs in the T2SS and the T4bP system (30–32), would connect the cytoplasmic motor with the outer membrane secretin, allowing for the efficient transmission of the signals that control its opening and closing.

Interaction of the major pilin subunit with the periplasmic components PilNOP has been reported for the *N. meningitidis* T4P system (23) and for corresponding components of the T2SS (23, 33, 34) and the T4bP system (35). Our pulldown experiment from PAO1 lysates provides indirect evidence that a similar interaction occurs in *P. aeruginosa*. Based on the efficiency of the pulldown observed in our experiments (Fig. 6), the interaction of PilA with PilNOP may be transient. This scenario would be expected for a dynamic interaction where the PilA monomers encounter the PilNOP complex in transit to or from the pilus. One potential reason for PilA's interaction with the alignment complex (PilMNOP) is to transiently cluster pilin monomers at the polar site of pilus assembly, providing a high local concentration of PilA to promote rapid pilus assembly, and to prevent diffusion of PilA monomers away from the system following disassembly. Further, PilMNOP and the periplasmic domains of PilQ may participate in selection of the T4P major and minor pilins over the T2SS pseudopilins and minor pseudopilins, maintaining the fidelity of pilus composition and function. Finally, as the pilus experiences forces in excess of 100 pN upon retraction (4), PilA interaction sites in the periplasm could contribute to anchoring of the pilus. Indeed, the SS domain in the T4P-specific secretin (PilQ) may be a unique adaptation that could act as a clamp on the assembled fiber.

The T4P-specific interaction between Pro85 and Trp161 of PilP may also be important for the efficient generation of long retractable extracellular filaments. We suggest that this interaction is related to PilP's bridging of PilMNO in the inner membrane and PilQ in the outer membrane, and that maintaining the orientation of the disordered N terminus and β-sandwich domains of PilP is important for stabilizing the PilMNOPQ complex *in vivo*. Also, the SS domains in PilQ (absent from the T2SS secretins) may constrain the dynamics of the PilPQ interaction, and the Pro85-Trp161 tether may promote an optimal PilPQ interface.

The full T4P transenvelope complex is unlikely to have a closed lumen like that in the T3SS needle complex (36, 37), since addition and removal of PilA subunits at the periplasmic face of the inner membrane are absolutely required for pilus extension and retraction to occur. Our earlier work indicated that PilNOP interact in a 1:1:1 complex (12), and the PilMN interaction suggests a 1:1 stoichiometry as well (9). Recent structural studies of T2SS and T4P components further suggest that PilP and PilQ form a 1:1 interaction, and comparison of the available data regarding this heterodimeric interface suggests that this organization is conserved between the two systems (6, 22). Also, when the N-terminal domain of PilP is attached to the inner membrane via its lipid anchor and interacting with PilNO, the nature of the Pro85-Trp161 interaction would position the PilQ interaction interface on PilP up, toward the outer membrane, possibly facilitating the

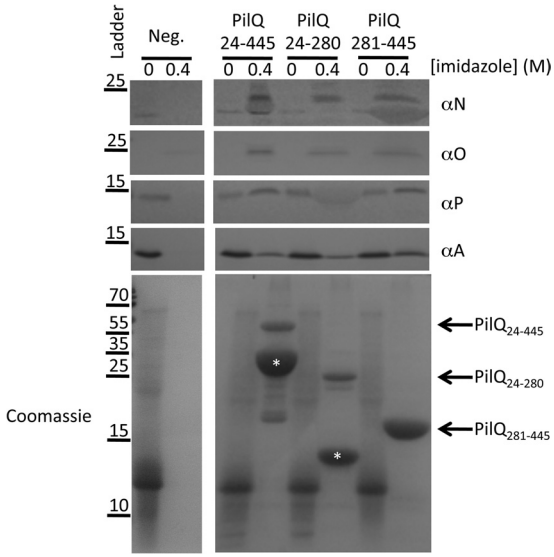

FIG 6 Periplasmic regions of PilQ pull down PilA. After binding various $PilQ_{6\times His}$ constructs on a Ni-NTA column, the flowthrough (0 M imidazole) and highest elution (0.4 M imidazole) fractions were examined by Coomassie staining and with PilN-, PilO-, PilP-, or PilA-specific antibodies. The locations of the molecular mass markers are shown as labeled bars on the left side of the figure (in kDa). The locations of the PilQ constructs in the 0.4 M imidazole elution fractions are shown by arrows at the right of the figure, and white asterisks denote PilQ degradation products.

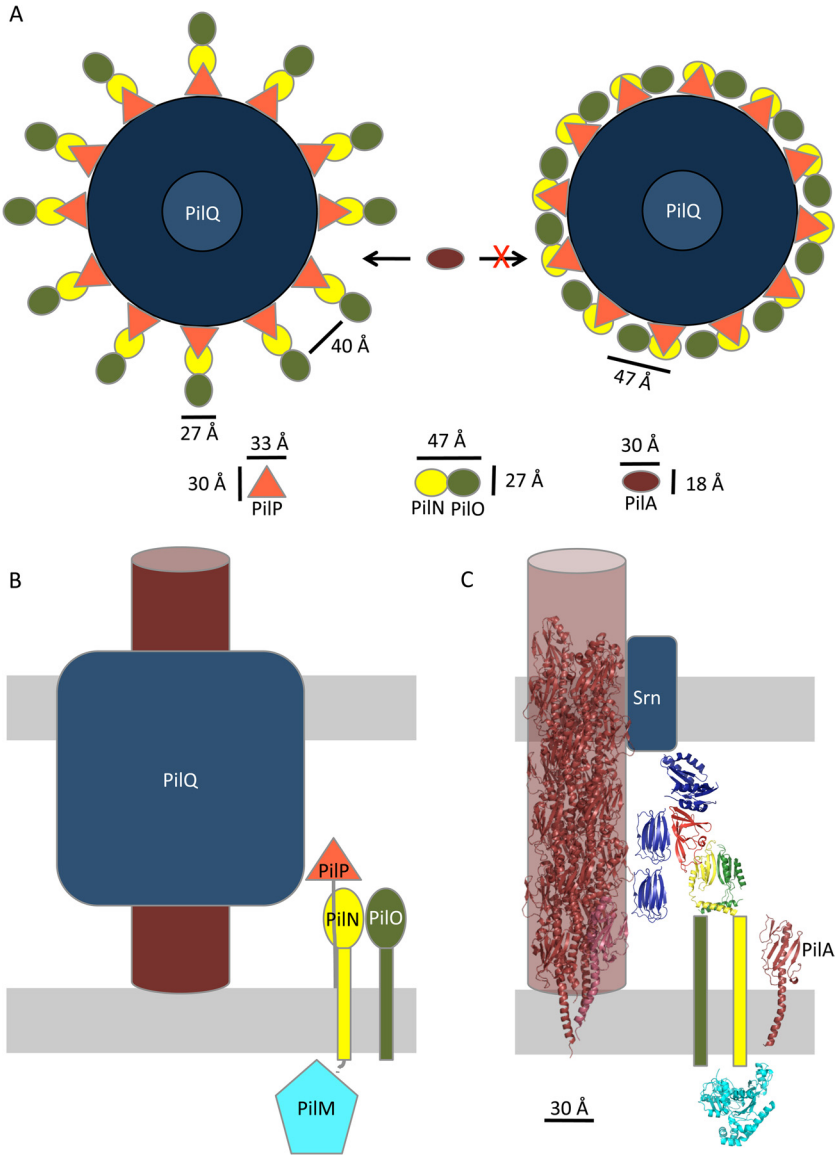

FIG 7 Model of the PilMNOPQ transenvelope complex. (A) Scale schematic of T4P complex and possible orientations of periplasmic components (top-down orientation). The circumference of the PilQ pore is approximately 575 Å. PilN, PilO, PilP, and PilQ are drawn to scale. PilM, which is omitted for clarity as it is located in the cytoplasm, is believed to interact with PilN with a 1:1 stoichiometry. The left panel depicts the narrow face of PilNOP adjacent to the pore, while the right panel depicts the wide edge of PilNOP adjacent to the pore. (B) Schematic representation of the PilMNOPQ complex approximately to scale. (C) Scale model using experimentally determined or modeled structures for PilMNOP and PilA, a homology model for the N0 and N1 domains, and the structure of the B2 domain of *N. meningitidis* (PDB code 4AQZ) for SS1 and SS2. The orientation of PilP and the N0 domain of PilQ was achieved by overlaying the $PilP_{\Delta 71}$ and the homology model of PilQ N0 and N1 domains on the C and D chains of the GspC/D cocrystal structure (PDB code 3OSS). Scale and coloring are as shown for panel B. For PilQ, the size of the secretin (Srn) domain is estimated based on the size of the N0 and N1 domains.

PilPQ interaction. In this orientation, one could imagine a series of rings through the periplasm, where PilNO form a ring closest to the inner membrane, PilP forms a ring above PilNO, and PilQ forms a ring closest to the outer membrane, extending downward into the periplasm (Fig. 7B and C). Since PilQ is predicted to be a dodecameric complex (6), there could be 12 PilMNOPQ units arranged in a circular manner, similar to the arrangement in T2SS, T3SS, and T4SS assembly complexes (37–39) (Fig. 7). Alternatively, data from the T2SS suggests that the secretin is assembled as a hexamer of dimers (40–42); in this case, the arrangement may be one PilMNOP complex for every two PilQ monomers (1:1:1:1:2 stoichiometry). Differences in orientation of the N0 domain of PilQ in a dimer versus monomer configuration might explain why we saw differences in PilPQ interactions when fragments versus full periplasmic domains of PilQ were used for pulldowns.

The requirement for addition and removal of PilA subunits at the periplasmic face of the inner membrane means that the periplasmic constituents likely are arranged in a way that allows room for this process. Using the dimensions of the structures determined by nuclear magnetic resonance (NMR), X-ray crystallography, and electron microscopy for PilNOPQ (11, 12, 43), a scale model showing the putative arrangement of periplasmic

components can be derived (Fig. 7A). The outer diameter of the *P. aeruginosa* PilQ secretin was measured from negatively stained PilQ complexes to be ~183 Å (43), leading to a circumference of 575 or ~48 Å per monomer in a dodecamer. When viewed from above, the β-sandwich domain of PilP is ~33 by ~30 Å, and the dimensions of the ferredoxin-like fold of a PilNO heterodimer (based on the fragment of PilO that was determined by X-ray crystallography) are ~47 by 27 Å. As the N terminus of PilP facilitates the PilNOP interaction, it is unlikely to substantially affect the width of a PilNOP complex. If 12 PilNO heterodimers are oriented with the broad (47-Å) face facing the conduit, there would be no room for the lateral introduction of PilA monomers (Fig. 7A, right). However, if PilNO are oriented with the narrow (27 Å) face toward the conduit, there is ample room for entry and exit of PilA (~30 by 18 Å) in the gap between PilNOP complexes (~40 Å) (Fig. 7A, left). There are five major pilin subtypes in *P. aeruginosa* (44), with head groups of various sizes (45), supporting the need for a large enough gap between the spokes formed by the PilMNOP transenvelope complex to accommodate structurally distinct pilins and, likely, the minor pilins as well. Alternatively, if there is one PilMNOP complex per PilQ dimer, there would be sufficient space between the PilMNOP spokes, regardless of the orientation of PilNOP, to facilitate the addition and removal of pilin and minor pilin monomers.

Drawing the components to scale and including available structures (Fig. 7B), it is clear that the SS domain of PilQ extends a significant distance across the periplasm toward the inner membrane. As has been suggested elsewhere (46), we propose that the periplasmic region of PilQ forms the inside of the channel, while the PilMNOP subcomplex forms the exterior. In this arrangement, both PilMNOP and PilQ could interact with monomeric PilA and/or the minor pilins. This interaction could serve a number of roles, including concentrating the pilin subunits at the site of assembly/disassembly, communicating assembly/disassembly signals from the cytoplasm to the PilA subunits, or stimulating opening of the secretin. The SS domains of PilQ could be involved in the initial stages of polymerization (through as-yet uncharacterized interactions with a priming complex) and/or clamping on the pilus to ensure it remains anchored in the membrane under tension. In our favored model, the transenvelope complex, composed of PilMNOPQ, is a stable assembly through the cell envelope, while the signal(s) for assembly/disassembly of the pilus come from the communication between the cytoplasmic motor complex (made up of the platform protein PilC [47] and the ATPases PilB/T/U) and PilM. Further studies are needed to better understand the nature of the communication between the motor and alignment subcomplexes and the exact mechanism of PilA polymerization/depolymerization. With this work, we have provided a framework for the further examination of these processes.

ACKNOWLEDGMENTS

This work was supported by Operating Grant MOP 93585 from the Canadian Institutes of Health Research (CIHR) to L.L.B. and P.L.H. J.K. and S.T. have been funded, in part, by graduate scholarships from CIHR and Cystic Fibrosis Canada, respectively. P.L.H. is the recipient of a Canada Research Chair.

REFERENCES

1. **Bradley DE.** 1973. Basic characterization of a *Pseudomonas aeruginosa* pilus-dependent bacteriophage with a long noncontractile tail. J. Virol. **12**:1139–1148.
2. **Bradley DE.** 1974. The adsorption of pilus-dependent bacteriophages to a host mutant with nonretractile pili. Virology **58**:149–163.
3. **Burrows LL.** 2005. Weapons of mass retraction. Mol. Microbiol. **57**:878–888.
4. **Maier B, Potter L, So M, Long CD, Seifert HS, Sheetz MP.** 2002. Single pilus motor forces exceed 100 pN. Proc. Natl. Acad. Sci. U. S. A. **99**:16012–16017.
5. **Burrows LL.** 2012. Pseudomonas aeruginosa twitching motility: type IV pili in action. Annu. Rev. Microbiol. **66**:493–520.
6. **Berry J-L, Phelan MM, Collins RF, Adomavicus T, Tonjum T, Frye SA, Bird L, Owens RJ, Ford RC, Lian L-Y, Derrick JP.** 2012. Structure and assembly of a trans-periplasmic channel for type IV pili in *Neisseria meningitidis*. PLoS Pathog. **8**:e1002923. doi:10.1371/journal.ppat.1002923.
7. **Koo J, Tammam SD, Ku S-Y, Sampaleanu L, Burrows LL, Howell PL.** 2008. PilF is an outer membrane lipoprotein required for multimerization and localization of the *Pseudomonas aeruginosa* type IV pilus secretin. J. Bacteriol. **190**:6961–6969.
8. **Ayers M, Sampaleanu L, Tammam SD, Koo J, Harvey H, Howell PL, Burrows LL.** 2009. PilM/N/O/P proteins form an inner membrane complex that affects the stability of the *Pseudomonas aeruginosa* type IV pilus secretin. J. Mol. Biol. **394**:128–142.
9. **Karuppiah V, Derrick JP.** 2011. Structure of the PilM-PilN inner membrane type IV pilus biogenesis complex from *Thermus thermophilus*. J. Biol. Chem. **286**:24434–24442.
10. **Yamagata A, Milgotina E, Scanlon Craig KL, Tainer JA, Donnenberg MS.** 2012. Structure of an essential type IV pilus biogenesis protein provides insights into pilus and type II secretion systems. J. Mol. Biol. **419**:110–124.
11. **Sampaleanu LM, Bonanno JB, Ayers M, Koo J, Tammam S, Burley SK, Almo SC, Burrows LL, Howell PL.** 2009. Periplasmic domains of *Pseudomonas aeruginosa* PilN and PilO form a stable heterodimeric complex. J. Mol. Biol. **394**:143–159.
12. **Tammam S, Sampaleanu LM, Koo J, Sundaram P, Ayers M, Chong PA, Forman-Kay JD, Burrows LL, Howell PL.** 2011. Characterization of the PilN, PilO and PilP type IVa pilus subcomplex. Mol. Microbiol. **82**:1496–1514.
13. **Giltner CL, Habash M, Burrows LL.** 2010. *Pseudomonas aeruginosa* minor pilins are incorporated into type IV pilus. J. Mol. Biol. **398**:444–461.
14. **Ayers M, Howell PL, Burrows LL.** 2010. Architectures of the type II secretion and type IV pilus machineries. Future Microbiol. **5**:1203–1218.
15. **Peabody CR, Chung YJ, Yen Vidal-Ingigliardi M-RD, Pugsley AP, Saier MHJ.** 2003. Type II protein secretion and its relationship to bacterial type IV pili and archael flagella. Microbiology **149**:3051–3072.
16. **Russel M.** 1998. Macromolecular assembly and secretion across the bacterial cell envelope: type II protein secretion systems. J. Mol. Biol. **279**:485–499.
17. **Abendroth J, Kreger AC, Hol WG.** 2009. The dimer formed by the periplasmic domain of EpsL from the type 2 secretion system of *Vibrio parahaemolyticus*. J. Struct. Biol. **168**:313–322.
18. **Abendroth J, Bagdasarian M, Sandkvist M, Hol WGJ.** 2004. The structure of the cytoplasmic domain of EpsL, an inner membrane component of the type II secretion system of *Vibrio cholerae*: an unusual member of the actin-like ATPase superfamily. J. Mol. Biol. **344**:619–633.
19. **Abendroth J, Murphy P, Sandkvist M, Bagdasarian M, Hol WGJ.** 2005. The X-ray structure of the type II secretion system complex formed by the N-terminal domain of EpsE and the cytoplasmic domain of EpsL of *Vibrio cholerae*. J. Mol. Biol. **348**:845–855.
20. **Sandkvist M, Keith JM, Bagdasarian M, Howard SP.** 2000. Two regions of EpsL involved in species-specific protein-protein interactions with EpsE and EpsM of the general secretion pathway in *Vibrio cholerae*. J. Bacteriol. **182**:742–748.
21. **Gu S, Kelly G, Wang X, Frenkiel T, Shevchik VE, Pickersgill RW.** 2012. Solution structure of the HR domain of the type II secretion system. J. Biol. Chem. **287**:9072–9080.
22. **Korotkov KV, Johnson TL, Jobling MG, Pruneda J, Pardon E, Héroux A, Turley S, Steyaert J, Holmes RK, Sandkvist M, Hol WGJ.** 2011. Structural and functional studies on the interaction of GspC and GspD in the type II secretion system. PLoS Pathog. **7**:e1002228. doi:10.1371/journal.ppat.1002228.
23. **Georgiadou M, Castagnini M, Karimova G, Ladant D, Pelicic V.** 2012. Large-scale study of the interactions between proteins involved in type IV

pilus biology in *Neisseria meningitidis*: characterization of a subcomplex involved in pilus assembly. Mol. Microbiol. **84**:857–873.
24. **Balasingham SV, Collins RF, Assalkhou R, Homberset H, Frye SA, Derrick JP, Tonjum T.** 2007. Interactions between the lipoprotein PilP and the secretin PilQ in *Neisseria meningitidis*. J. Bacteriol. **189**:5716–5727.
25. **Notredame C, Higgins DG, Heringa J.** 2000. T-Coffee: a novel method for fast and accurate multiple sequence alignment. J. Mol. Biol. **302**:205–217.
26. **Waterhouse AM, Procter JB, Martin DMA, Clamp M, Barton GJ.** 2009. Jalview version 2–a multiple sequence alignment editor and analysis workbench. Bioinformatics **25**:1189–1191.
27. **Cole C, Barber JD, Barton GJ.** 2008. The Jpred 3 secondary structure prediction server. Nucleic Acids Res. **36**:W197–W201.
28. **DeLano WL.** 2002. The PyMOL molecular graphics system. DeLano Scientific, San Carlos, CA.
29. **Genin S, Boucher CA.** 1994. A superfamily of proteins involved in different secretion pathways in Gram-negative bacteria: modular structure and specificity of the N-terminal domain. Mol. Gen. Genet. **243**:112–118.
30. **Arts J, de Groot A, Ball G, Durand E, Khattabi ME, Filloux A, Tommassen J, Koster M.** 2007. Interaction domains in the *Pseudomonas aeruginosa* type II secretory apparatus component XcpS (GspF). Microbiology **153**:1582–1592.
31. **Py B, Loiseau L, Barras F.** 2001. An inner membrane platform in the type II secretion machinery of Gram-negative bacteria. EMBO Rep. **2**:244–248.
32. **Milgotina EI, Lieberman JA, Donnenberg MS.** 2011. The inner membrane subassembly of the enteropathogenic *Escherichia coli* bundle-forming pilus machine. Mol. Microbiol. **81**:1125–1127.
33. **Lee M-S, Chen L-Y, Leu W-M, Shiau R-J, Hu N-T.** 2005. Associations of the major pseudopilin XpsG with XpsN (GspC) and secretin XpsD of *Xanthomonas campsetris pv. campestris* type II secretion apparatus revealed by cross-linking analysis. J. Biol. Chem. **280**:4585–4591.
34. **Gray MD, Bagdasarian M, Hol WGJ, Sandkvist M.** 2011. *In vivo* cross-linking of EpsG to EpsL suggests a role for EpsL as an ATPase-pseudopilin coupling protein in the type II secretion system of *Vibrio cholerae*. Mol. Microbiol. **79**:786–798.
35. **Hwang J, Bieber D, Ramer SW, Wu C-Y, Schoolnik GK.** 2003. Structural and topographical studies of the type IV bundle-forming pilus assembly complex of enteropathogenic *Escherichia coli*. J. Bacteriol. **185**:6695–6701.
36. **Blocker A, Jouihri N, Larquet E, Gounon P, Ebel F, Parsot C, Sansonetti P, Allaoui A.** 2001. Structure and composition of the *Shigella flexneri* "needle complex," a part of its type III secreton. Mol. Microbiol. **39**:652–663.
37. **Schraidt O, Marlovits TC.** 2011. Three-dimensional model of Salmonella's needle complex at subnanometer resolution. Science **331**:1192–1195.
38. **McLaughlin LS, Haft RJ, Forest KT.** 2012. Structural insights into the type II secretion nanomachine. Curr. Opin. Struct. Biol. **22**:208–216.
39. **Fronzes R, Scharer E, Wang L, Saibil H, Orlova EV, Waksman G.** 2009. Structure of a type IV secretions system core complex. Science **323**:266–268.
40. **Van der Meeren R, Wen Y, Van Gelder P, Tommassen J, Devreese B, Savvides SN.** 2013. New insights into the assembly of bacterial secretins: structural studies of the periplasmic domain of XcpQ from *Pseudomonas aeruginosa*. J. Biol. Chem. **288**:1214–1225.
41. **Wang X, Pineau C, Gu S, Guschinskaya N, Pickersgill RW, Shevchik VE.** 2012. Cysteine scanning mutagenesis and disulfide mapping analysis of the arrangement of GspC and GspD protomers within the T2SS. J. Biol. Chem. **287**:19082–19093.
42. **Lieberman JA, Frost NA, Hoppert M, Fernandes PJ, Vogt SL, Raivio TL, Blanpied TA, Donnenberg MS.** 2012. Outer membrane targeting, ultrastructure and single molecule localization of the enteropathogenic *Escherichia coli* type IV pilus secretin BfpB. J. Bacteriol. **194**:1646–1658.
43. **Bitter W, Koster M, Latijnhouwers M, de Cock H, Tommassen J.** 1998. Formation of oligomeric rings by XcpQ and PilQ, which are involved in protein transport across the outer membrane of *Pseudomonas aeruginosa*. Mol. Microbiol. **27**:209–219.
44. **Kus JV, Tullis E, Cvitkovitch DG, Burrows LL.** 2004. Significant differences in type IV pilin allele distribution among *Pseudomonas aeruginosa* isolated from cystic fibrosis (CF) versus non-CF patients. Microbiology **150**:1315–1326.
45. **Nguyen Y, Jackson SG, Aidoo F, Junop M, Burrows LL.** 2010. Structural characterization of novel *Pseudomonas aeruginosa* type IV pilins. J. Mol. Biol. **395**:491–503.
46. **Douzi B, Ball G, Cambillau C, Tegoni M, Voulhoux R.** 2011. Deciphering the Xcp *Pseudomonas aeruginosa* type II secretion machinery through multiple interactions with substrates. J. Biol. Chem. **286**:40792–40801.
47. **Takhar HK, Kemp K, Kim M, Howell PL, Burrows LL.** 2013. The platform protein is essential for type IV pilus biogenesis. J. Biol. Chem. doi:10.1074/jbc.M113.453506.